Supplemental information

Hsp90 Regulation of Fibroblast Activation in Pulmonary Fibrosis

Vishwaraj Sontake [1, 4], Yunguan Wang[2], Rajesh K. Kasam[1, 4], Debora Sinner[3], Geereddy B. Reddy[4], Anjaparavanda P. Naren[1], Francis X. McCormack[5], Eric S. White[6], Anil G. Jegga[2, *], and Satish K. Madala[1, *]

[1]Division of Pulmonary Medicine, [2]Division of Biomedical Informatics and [3]Division of Neonatology and Pulmonary Biology, Cincinnati Children's Hospital Medical Center, Cincinnati, Ohio USA.

[4]Department of Biochemistry, National Institute of Nutrition, Hyderabad, Telangana, India.

[5]Division of Pulmonary, Critical Care and Sleep Medicine, University of Cincinnati, Cincinnati, Ohio USA.

[6]Department of Internal Medicine, University of Michigan Health System, Ann Arbor, Michigan, USA.

* Corresponding authors: Dr. Satish K. Madala, Division of Pulmonary Medicine, Cincinnati Children's Hospital Medical Center, 3333 Burnet Avenue, MLC 2021, Cincinnati, OH, 45229, USA Telephone: 513-636-9852 FAX: 513-636-3723. E-mail: satish.madala@cchmc.org

Dr. Anil G. Jegga, Division of Biomedical informatics, Cincinnati Children's Hospital Medical Center, 240 Albert Sabin Way, MLC 7024, Cincinnati, OH, 45229, USA Telephone: 513-636-0261 FAX: 513-636-2056. E-mail: anil.jegga@cchmc.org

Authorship note: A.G.J and A.K. M. are co-senior authors.

Conflict of interest: The authors have declared that no conflict of interest exists.

Methods

Human and mouse primary lung fibroblasts cultures. Human primary lung fibroblast cell cultures were prepared as previously described (1, 2). Lung tissue was collected into DMEM supplemented to contain 10% FBS and 1% each of penicillin, streptomycin, and amphotericin. Each lung-tissue sample was cut into 2 x 2 cm pieces, and each piece was finely minced and digested in 5 ml DMEM containing collagenase (2 mg/ml), incubated at 37°C for 1h. Digested tissues were passed through a 100-mm filter, washed twice by centrifugation at 1000 x g for 5 min, plated onto 100-mm tissue culture plates in 10 ml DMEM, and incubated at 37°C, 5% CO_2 to allow the cells to adhere and migrate away from the larger remaining tissue pieces. Unbound cells were removed on Day 2 of culture by washing cells with fresh DMEM. Adherent lung fibroblasts were cultured until confluent (1–2 wk). Similarly, mouse lung tissues were minced and cultured in IMDM supplemented with 5% FBS and 1% each of penicillin, streptomycin as previously described (1).

Myofibroblast transformation. To assess the effects of 17-AAG on fibroblast to myofibroblast transformation, primary mouse lung fibroblasts isolated from SMAcreER/ROSA mTmG/+ mice were seeded on to chamber slides at density of $1x10^5$ for 24h. Cells were serum starved (0.5% FBS) at 70–80% confluency for overnight and then treated with 2μM 4-hydroxytamoxifen (Cat# H7904, sigma-Aldrich, ST. Louis. MO, USA) for 72 h in presence or absence of TGFβ (20 ng/ml) or 17-AAG (0.2μM). For genetic knockdown studies cells grown on chamber slides were transfected with control or Hsp90AA or Hsp90AB siRNA for 24h, post transfection cells were treated with 2μM 4-hydroxytamoxifen in presence and absence of TGFβ for additional 72h. After 72h, cells were fixed with 4% paraformaldehyde and the nucleus was stained using prolong gold DAPI. Fluorescence images were collected using a Nikon AIR-A1 laser-scanning confocal microscope (Melville, NY, USA). For quantitation of SMAcreER induced green positive cells, 5-6 random images were taken for each condition (DMSO or TGFβ or TGFβ and 17-AAG) with the 10X or 20X objective. Cell quantitation was performed using Metamorph imaging software.

TGFβ stimulation and 17-AAG treatment. To assess the effects of 17-AAG on TGFβ-induced ECM expression, primary fibroblasts from non-IPF controls were plated in 24-well plates at a density of $1.5x10^5$

cells/well and cultured to reach 70–80% confluency. Cells were then serum starved (0.5% FBS) for 24h, pretreated with 17-AAG for 2h, and then stimulated with recombinant human TGFβ (20 ng/ml; R&D Systems) in the presence or absence of 17-AAG for 24h. After 24h of stimulation, cells were lysed in RLT lysis buffer supplemented with β-mercaptoethanol for RNA isolation and cDNA synthesis. Quantitative PCR analyzed ECM gene expression.

Fibroblast and fibrocyte invasion and migration. In vitro invasion and migration assays were performed using human or mouse primary lung-resident fibroblasts ($CD45^-Col1^+$) or fibrocytes ($CD45^+Col1^-$), isolated as described previously (1, 3). 96-well Image Lock plates (Essen Biosciences) were used for all experiments. Invasion assay plates were coated with BD matrigel (50 µl/well; 100 µg/ml in IMDM) and incubated at 37°C, 5% CO_2 for overnight. Day 2 wells were washed twice with media (0.5% FCS) (2x100 µl/well). Lung-resident fibroblasts or fibrocytes (50k/well) were seeded and grown to form a confluent monolayer (37°C, 5% CO_2, one day). Scratch wounds were made on Day 3 using a 96-well pin wound-maker according to the manufacturer instructions (Essen Biosciences, Ann Arbor, Michigan, USA). Plates were washed twice with media (0.5% FCS) (2x100 µl/well). Matrigel containing 17-AAG or DMSO (50 µl/well; 3 mg/ml) was added on top of the cell layer to fill in the wound area with matrigel and incubated at 37°C, 5% CO_2 for 30 min. Invasion through matrigel is used to mimic the invasion process through ECM that is similar in composition to lung basement membrane. Additional (100 µl/well) media with or without 17-AAG was added and placed in IncuCyte ZOOM for heigh-content imaging. For migration assay, plates were precoated with fibronectin (50 µl/well; 10 µg/ml in PBS) for 2h. Lung resident fibroblasts or fibrocytes (50 k/well) were seeded and grown to form a confluent monolayer (37°C, 5% CO_2, one day). Scratch wounds were made on Day 2, and plates were washed twice with media (0.5% FCS) (2x100 µl/well). Migration was assessed in the presence and absence of 17-AAG or by genetic knockdown of Hsp90AA or Hsp90AB siRNA using the IncuCyte ZOOM height-content imaging system as previously described (3).

Immunoprecipitation and Hsp90 ATPase assay. Lung tissue lysates from control or TGFα mice were prepared in HEPES lysis buffer (20 mM HEPES, pH 7.3, 1 mM EDTA, 5 mM Mg Cl_2, 100 mM KCl) supplemented with

protease inhibitors and cleared by centrifugation at 10,000 rpm. Pre-conjugated anti-Hsp90 protein-A/G agarose beads were incubated with 50 µl of tissue lysates (tissue lysates were pre-cleared with 50 µl of protein-A/G agarose beads; 50% slurry). The ATPase activity of the immunoprecipitated Hsp90 was measured by detection of free inorganic phosphate (Pi) release using a PiPer Phosphate Assay Kit (Molecular Probes, Cat# P22061). The assay measures an increase in absorption at 565 nm of an Amplex Red reagent, which is proportional to the amount of Pi in the sample, and activity of Hsp90 was represented as an increase in absorbance at 3h.

Hsp90 affinity binding assay. Primary fibroblasts cell lysates from control or TGFα mice were prepared in HEPES lysis buffer (20 mM HEPES, pH 7.3, 1 mM EDTA, 5 mM $MgCl^2$, 100mM KCl) supplemented with protease inhibitors. The competitive binding assay was performed as described previously, with minor modifications (4). Protein lysates (50 µg) were incubated with increasing concentrations of 17-AAG or without 17-AAG for 1h at 4^{o}C, and then incubated with biotin-GM linked to BioMag streptavidin magnetic beads (Cat # 311711; Qiagen) for 1hr at 4^{o}C. Tubes were placed on a magnetic rack, and the unbound supernatant was removed. The magnetic beads were then washed three times with lysis buffer containing protease inhibitor and once with PBS. Samples were eluted in LDS sample buffer containing DTT, a reducing agent. Beads along with LDS were incubated at 70^{o}C for 10 min. Samples were then analyzed on LDS protein gels, and immunoblots were probed for Hsp90. Bands in the Western blots were quantified using the volume-integration function on Phosphor Imager software Image Quant 5.2 (Molecular Dynamics, Piscataway, NJ), and the percentage inhibition of binding of Hsp90 to the biotin-GM was calculated by assigning control as 100%.

Immunofluorescence. For the actin polymerization assay or PCNA immunostaining, lung-resident fibroblasts isolated from mouse or human primary lung-cell cultures were grown on glass coverslips overnight and treated with 17-AAG (1µM) or DMSO for 24h; then cells were fixed in 4% paraformaldehyde. Nonspecific protein binding was blocked with 3% BSA in PBS, followed by incubation with primary antibodies in blocking solution and subsequent incubation with secondary antibodies. Finally, the coverslips were washed and mounted on glass slides with Prolong gold DAPI. Confocal images were collected using a Nikon AIR-A1 laser-scanning confocal microscope (Melville, NY, USA). A z-stack of optical sections, 10 µm in total thickness, was captured from

DMSO- or 17-AAG-treated coverslips, and five 3D images were obtained per condition. Imaris (version 7.2.0; Bitplane, South Windsor, CT, USA) was used for colocalization analysis for Hsp90 and actin. For quantitative analysis of PCNA, 7-8 random images were taken for each condition (DMSO or 17-AAG) with the 10X objective. Cell quantitation was performed using Metamorph imaging software. PCNA levels were represented as percent proliferating cells in a given condition. Representative images were taken with the 60X oil objective, and data were reported as ± SEM of cell number for each experimental condition.

Hsp90 small interfering RNA transfection. Primary human or mouse lung-resident fibroblasts were transfected with Silencer Hsp90AA or Hsp90AB small interfering RNA (siRNA) (Cat # 4390771, Id # s67900 or s67899; Ambion) or silencer control siRNA (Cat # AM4611; Ambion) using the Lipofectamine 3000 Transfection kit (Invitrogen) according to the manufacturer's instructions. Primary lung-resident fibroblasts were separated from fibrocytes using anti-CD45 magnetic beads as described previously (1) and grown on 12-well plates to 90% confluence. Cells were transfected with siRNA using OptiMEM media containing no antibiotics. Transfected cells were harvested 72h post transfection and used for RNA isolation and gene-expression analysis.

BrdU incorporation. Primary lung-resident fibroblast proliferation was examined in the presence of 17-AAG or Hsp90AA or Hsp90AB siRNA using a colorimetric immunoassay based on BrdU incorporation using a BrdU Cell Proliferation Assay Kit (#6813, Cell Signaling Technology, Denver, USA) according to the manufacturer's instruction. In brief, CD45- Col+ primary resident fibroblasts (20,000 cells/well) were seeded in 96-well plates. Cells were incubated with different concentrations of 17-AAG (0.01, 0.05, 0.1, 0.5, and 1 μM) for 24h or transfected with Hsp90 siRNA for 48h, then 10 μl of 10X BrdU labeling solution was added in 100 μl of media per well and cells were incubated for an additional 24h. Post 24h BrdU labeling, cells were fixed and denatured using kit components, and immunodetection was performed as per the protocol recommended by manufacturer. Absorbance was taken at 450 nm, and proliferation was calculated as fold difference in proliferation over control.

RNA preparation and RT-PCR. Total RNA was extracted using the RNAeasy Mini Kit (Qiagen Sciences, Valencia, CA, USA) as previously described (1). cDNA synthesis was carried out using SuperScript® III Reverse Transcriptase (Invitrogen). qRT-PCR assays were performed with the CFX384 Touch Real-Time PCR Detection

system (Bio-Rad, Hercules, California, USA). The relative quantities of mRNA for several genes were determined using iTaq^{TM} universal SYBR green supermix (Bio-Rad). Target-gene transcripts in each sample were normalized to hypoxanthine guanine phosphoribosyl transferase or HPRT and expressed as a relative increase or decrease compared with control. All real-time primer sequences used are shown in Supplemental Tables 2 and 3.

Western blot. Purified lung resident fibroblasts ($CD45^{-}Col1^{+}$) were isolated as described, grown on 12-well plates to 90% confluence and treated with 17-AAG or DMSO for 48h. Cells were lysed in RIPA lysis buffer, and protein estimation was performed using the BCA method according to manufactures instructions (manufacturer information). Immunoblotting and quantification were performed using the volume-integration function of Phosphor Imager software Image Quant 5.2, as previously described (2). Primary antibodies and dilutions used are described in Supplemental Table 5, and the appropriate secondary antibodies conjugated with peroxidase (1:1000) were used for blot development.

Supplemental figure legends:

Supplemental Figure S1. 17-AAG attenuates migration and invasion. Primary Lung Fibroblast ($CD45^{-}$ $Col1^{+}$) and fibrocytes ($CD45^{+}$ $Col1^{+}$) were isolated from lung cultures of IPF lungs or TGF-α mice on Dox for 4wk. Scratch wound migration and invasion assay was performed in the presence and absence of 17-AAG (1μM) for 24h. **(A)** Quantitation of migration and invasion of fibroblasts isolated from lung cultures of TGF-α mice on Dox for 4wk and treated with vehicle of 17-AAG for 24h. **(B)** Quantitation of migration and invasion of fibrocytes isolated from lung cultures of IPF lungs and treated with vehicle of 17AAG for 24h. Data shown are mean ± SEM values. *$p<0.05$, **$p< 0.005$, ***$p<0.0005$.

Supplemental Figure S2. Hsp90AA and HSP90AB isoform-specific knockdown using siRNA. Primary lung fibroblasts ($CD45^{-}Col1^{+}$) were isolated from lung cultures of TGF-α mice on Dox for 4wk using anti-CD45 magnetic beads and transfected with either control- or Hsp90 isoform-specific siRNA for 72h. **(A, B)** Quantitation of Hsp90AA and Hsp90AB gene transcripts relative to Hprt in the lung fibroblasts of treated with control,

Hsp90AA or Hsp90AB-specific siRNA for 72h. Data represents two independent experiments with similar results. Data shown are mean ± SEM values (N = 3-6/group). **p<0.005 and ****p<0.00005.

Supplemental Figure S3. Limited or no effect of 17-AAG on genes involved in fibroblast migration. Primary lung fibroblasts ($CD45^{-}Col1^{+}$) were isolated from lung cultures of TGF-α mice on Dox for 4wk using anti-CD45 magnetic beads and treated with either vehicle or 17-AAG for 24h. The levels of Mmp2, Mmp9, and Timp2 gene transcripts relative to Hprt were quantified using qRT-PCR. Data is a representative of two independent experiments with similar results. Data shown are mean ± SEM values (N = 6/group).

Supplemental Figure S4. The effect of HSP90AA Knock down on Hsp90-driven genes involved in fibroproliferation in IPF. Primary lung fibroblasts ($CD45^{-}Col1^{+}$) were isolated from lung cultures of TGF-α mice on Dox for 4wk using anti-CD45 magnetic beads and transfected with either control- or Hsp90AA isoform-specific siRNA for 72h. The levels of Cdk4, Igf1, Mycn and Sphk1 gene transcripts relative to Hprt are quantified using qRT-PCR. Data is a representative of two independent experiments with similar results. Data shown are mean ± SEM values (N = 3-6/group).

Supplemental Figure S5. The effect of HSP90AA Knock down on Hsp90-driven ECM genes in IPF. Primary lung fibroblasts ($CD45^{-}Col1^{+}$) were isolated from lung cultures of TGF-α mice on Dox for 4wk using anti-CD45 magnetic beads and transfected with either control- or Hsp90AA isoform-specific siRNA for 72 hr. The levels of αSMA, Col1α, Col5α and FN1 gene transcripts relative to HPRT were quantified using qRT-PCR. Data is a representative of two independent experiments with similar results. Data shown are mean ± SEM (N = 3-6/group).

Supplemental Figure S6. The progressive expansion of fibrotic lesions during TGFα-induced pulmonary fibrosis. (A) Images of Masson's trichrome stained lung sections from control and TGFα mice on Dox for 3 or 6 wk. Scale bar, 200μm. Images are representative of each group with (N = 6-10/group). (B) Quantitation of the right lung weight of control and TGFα mice on Dox for 3 or 6 wk (N = 6-10/group). (C) Quantitation of total lung hydroxyproline levels in control and TGFα mice on Dox for 3 or 6 wk (N = 6-10/group). Statistical significance was measured using one-way ANNOVA with Sidak's multiple comparison test for all the experiments. ***p<0.0005 and ****p<0.00005**.**

Supplemental Figure S1

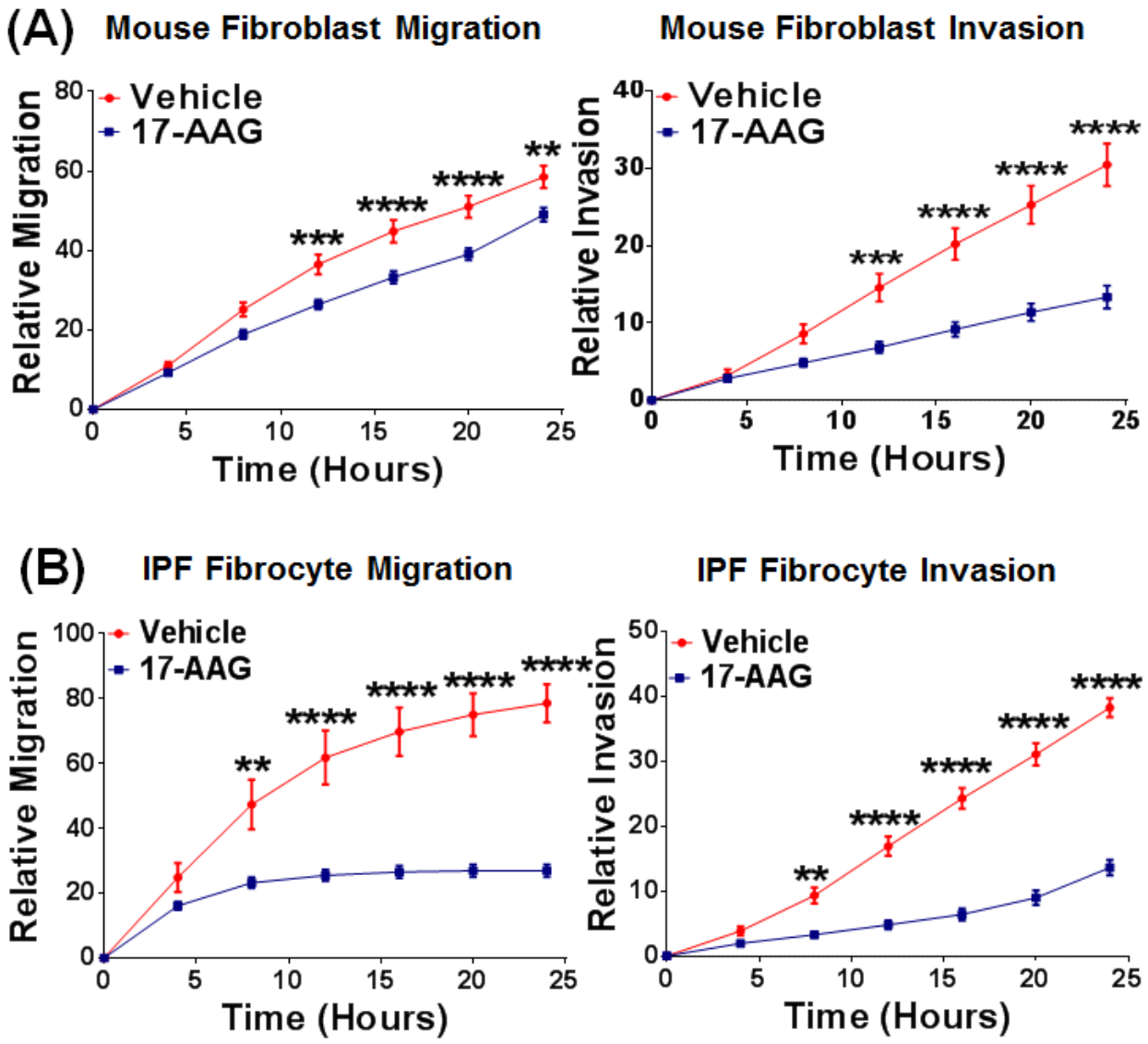

Supplemental Figure S2

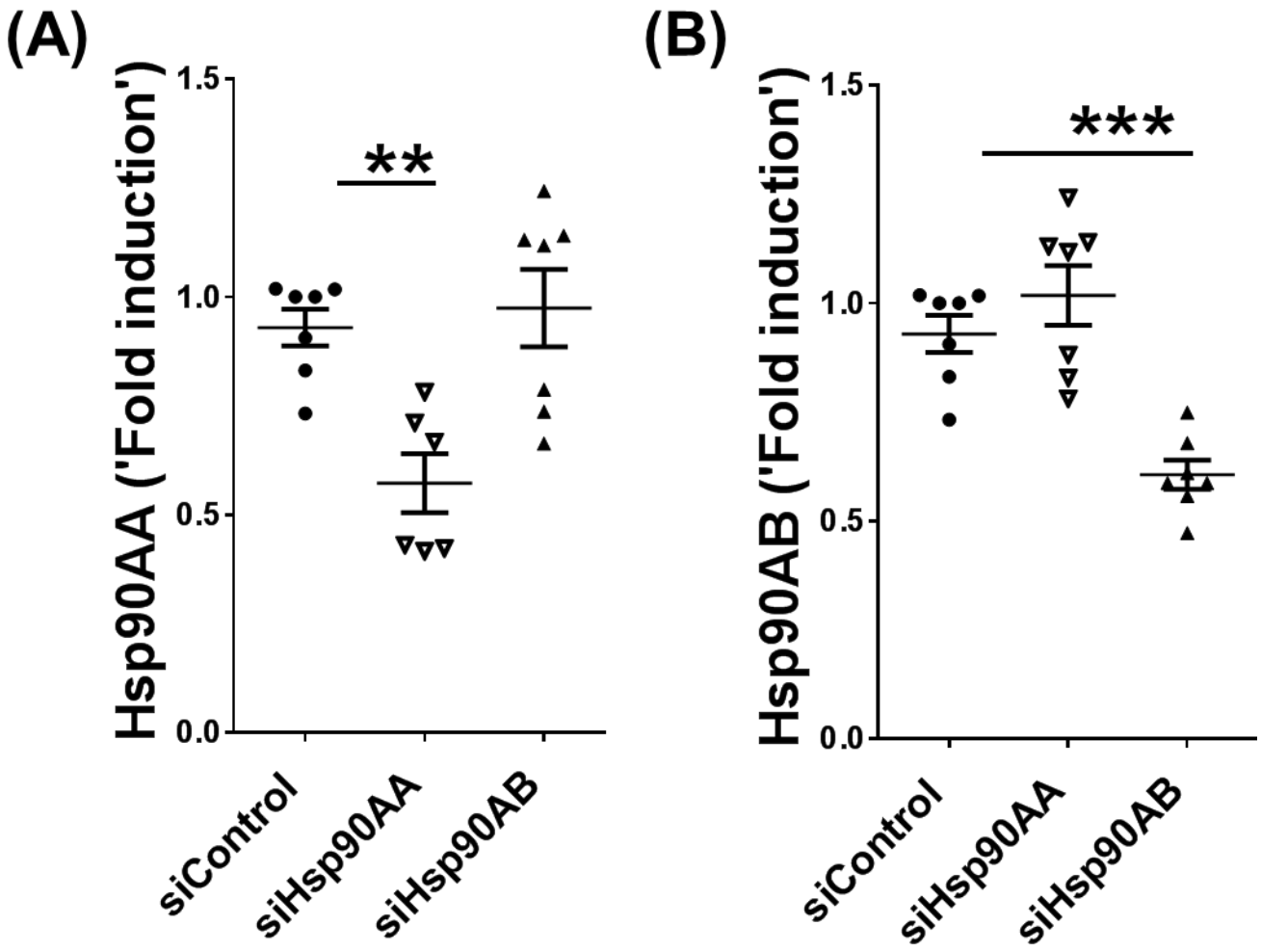

Supplemental Figure S3

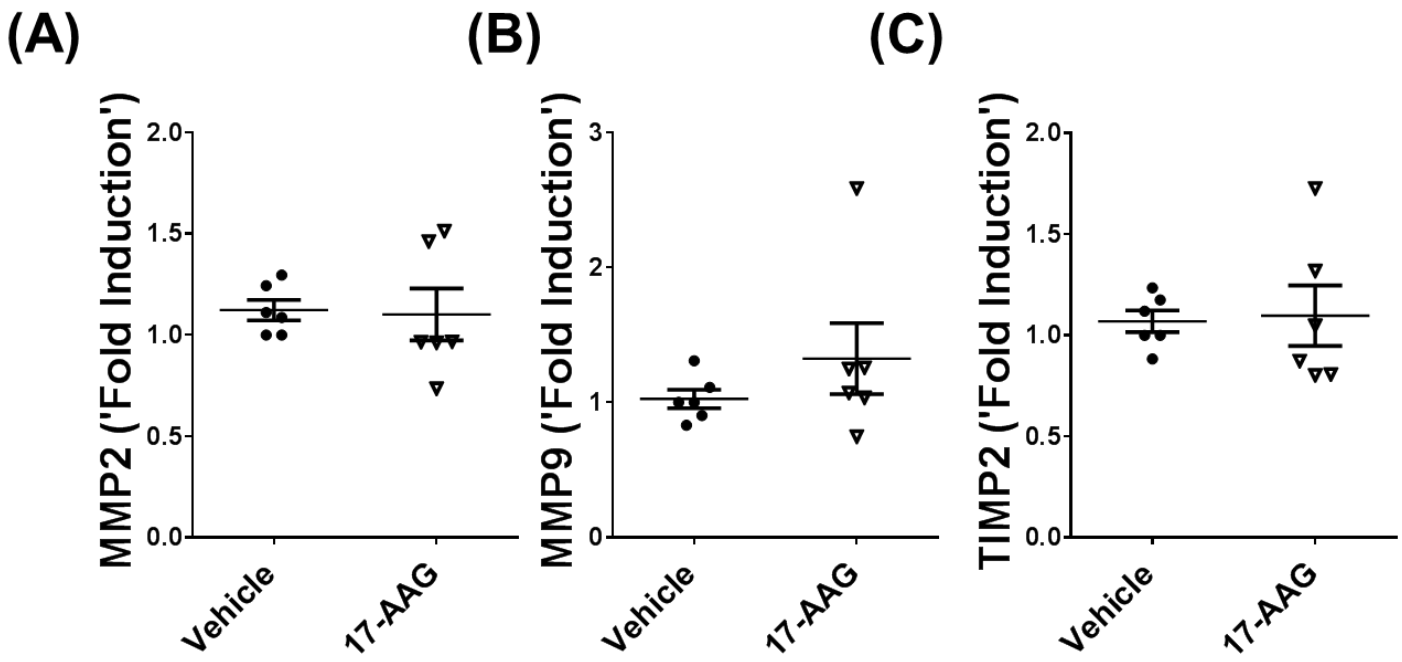

Supplemental Figure S4

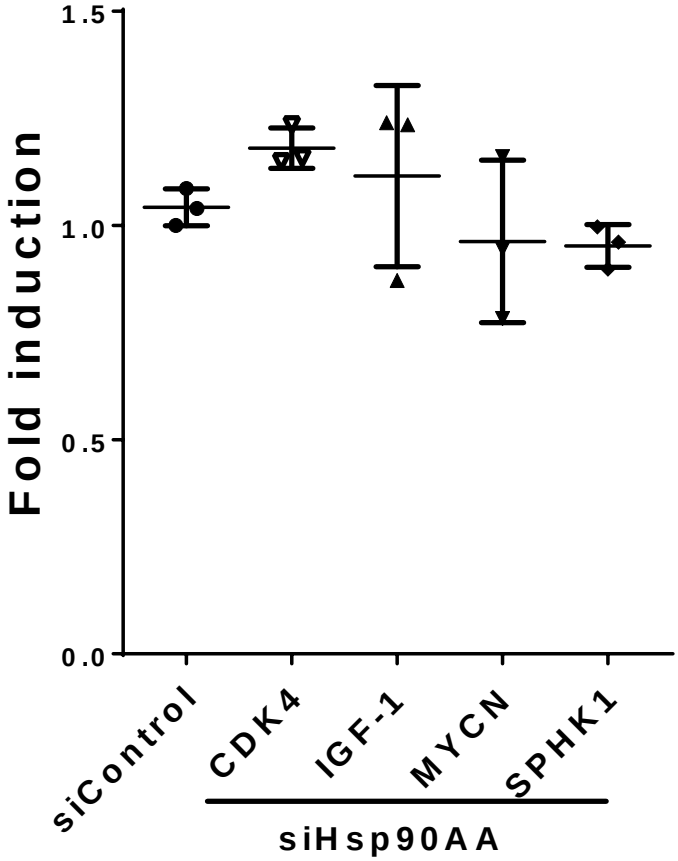

Supplemental Figure S5

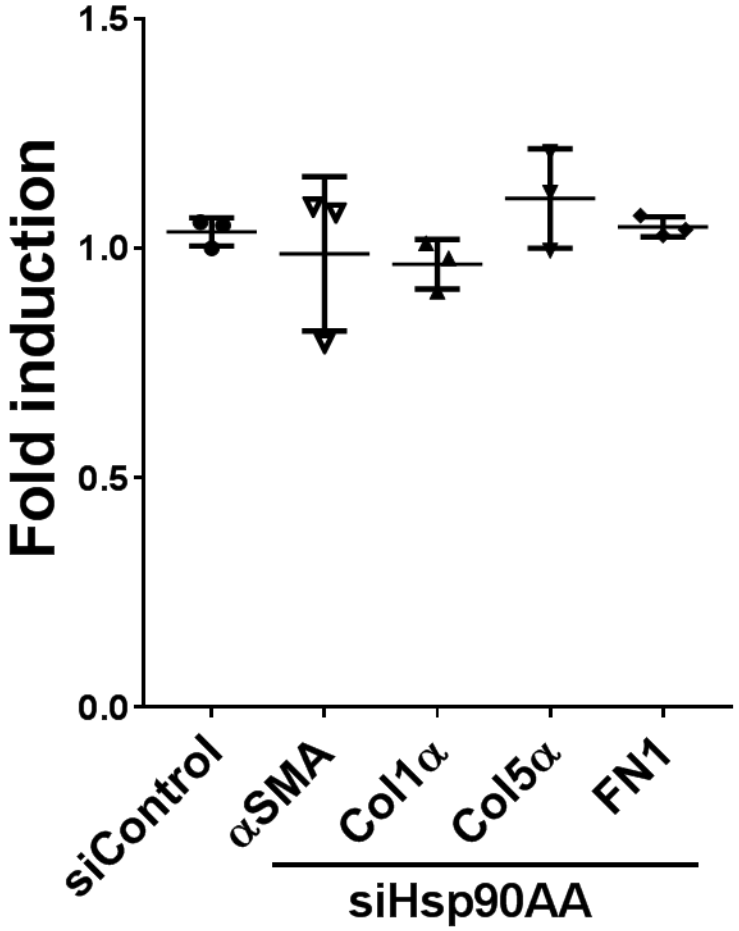

Supplemental Figure S6

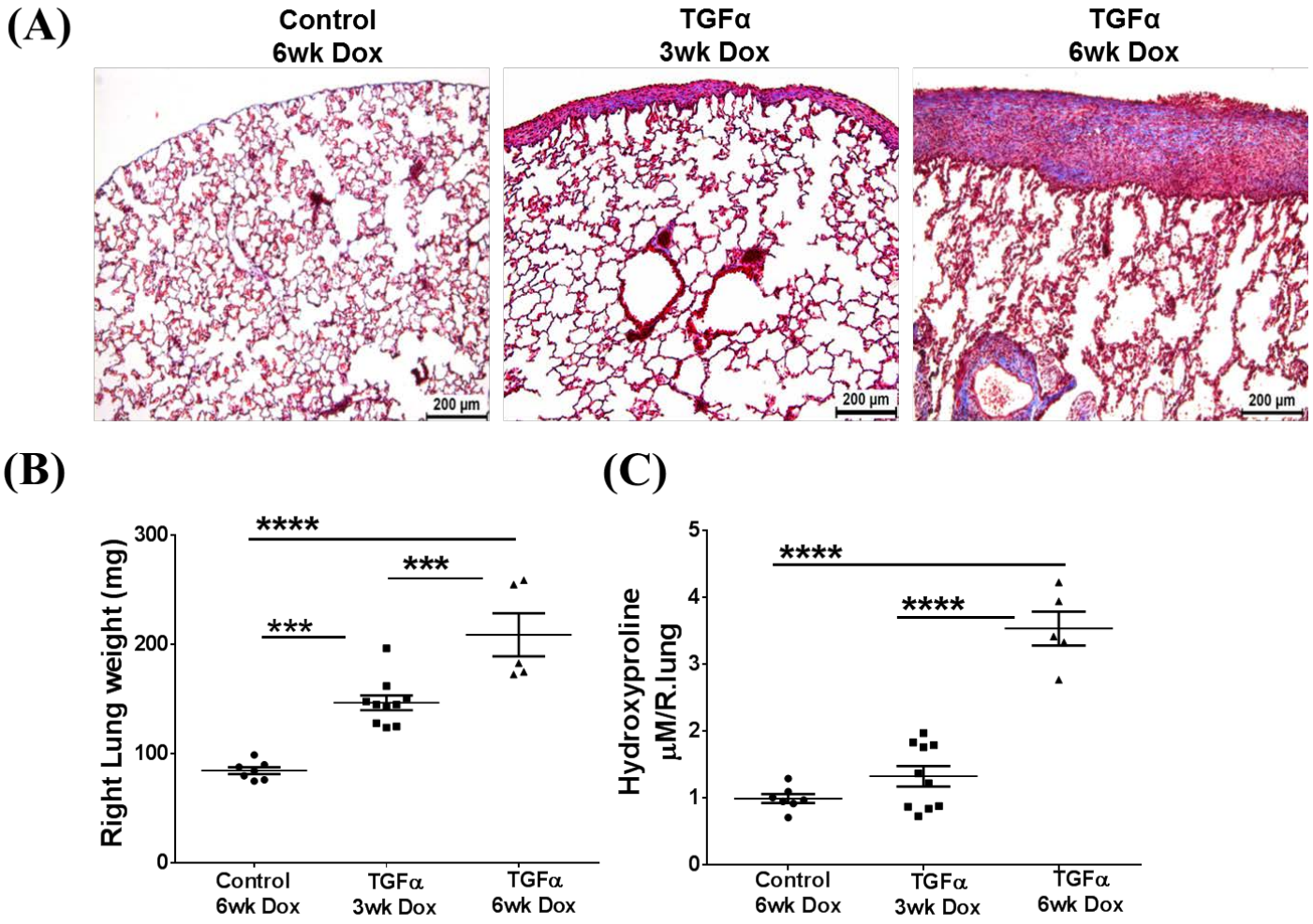

Supplemental Table 1. The list of IPF genes regulated by 17-AAG.

Genes Upregulated in IPF and Downregulated by 17-AAG	Genes Downregulated in IPF and Upregulated by 17-AAG
Gene Symbol	**Gene Symbol**
ABCC3	ABCC6
ADORA2B	ABHD6
AEN	ABL1
AK4	ACSM3
ALDH1A3	ACYP1
ANK2	ADD1
AQP3	ADRB2
ARL4C	AGTR1
ATP10B	AKAP9
BASP1	AKR1C1
BCL2A1	ALDH6A1
BCL3	ANG
BDKRB2	ARHGAP29
BIRC3	ARHGEF10
CCL2	ASL
CCL20	B3GNT2
CD24	BCL2L2
CD28	CALCOCO2
CDCP1	CCNB1IP1
CDKN1A	CDK19
CEMIP	CERS2
CFI	CES1
COCH	CIT
COL14A1	CLDN18
COL17A1	CLIC3
COL5A2	COBLL1
COL6A3	CYP3A5
CROT	DAPK1
CST1	DENND3
CTSG	DNM2
CTSK	DUSP8
CXCL12	EFNB2
CXCL13	EGFR
CXCL8	EMP2

DACT1	ENOSF1
DFNA5	ESRP2
DIO2	FAH
DIRAS3	FAM63A
DNM1	FASTKD1
DUSP4	FGGY
DUSP5	FLVCR2
DZIP1	GFOD1
EGR3	GGT1
ELF3	GLO1
EREG	GLUL
FAM102A	GNAQ
FAM69A	GPC3
FERMT1	GPM6B
FHL2	GPX3
FOSB	GSTM1
FOSL1	GTF3C3
FUT8	HBS1L
GALNT6	HIST1H4A
GATM	HMBOX1
GCNT3	HOXA5
GDF15	HTATIP2
GEM	IL1R2
GJB3	IL6ST
GM2A	IRS2
GNB5	IVD
GNL3	KAT6B
HIF1A	KIAA1109
HIST1H4J	KIF1C
HLA-DPB1	KLF9
HOMER3	KLHL24
HRH1	LAMA3
IER3	LAMA5
IGF1	MAN2A2
IL13RA2	MAP2K5
IL6	MAPK13
ITGA7	MAPK14
ITGB4	MAPT
JUNB	MAVS

KCNMA1	MFGE8
KCNN4	MKL2
KRT14	MKLN1
KRT6B	MT1E
KRT81	MT1H
LCN2	NDUFA10
LIF	NEDD4L
MEOX1	NPR3
MEX3C	OLFML2A
MMP11	PACSIN3
MMP7	PGC
MYC	PIR
NAMPT	PLCE1
NT5E	PPP1R13B
NTS	PPP3R1
OSBPL10	PRKAG2
PCSK1N	PRKCD
PDE1A	PRRG4
PFKP	PXMP4
PHLDA1	RAB11FIP1
PHLDA2	RAB11FIP2
PHTF2	RAB17
PLAU	RAD21
PLAUR	RAPGEF2
PLEK2	RASSF7
PMEPA1	RDX
POF1B	REPS2
PRKACB	RHOT1
PRR7	SACM1L
PRSS2	SAP30
PSD3	SCEL
PTGER4	SERPINA3
PTGS2	SESN1
RAB3B	SH3BP5
RND3	SHANK2
RNF19B	SLC26A2
SDC1	SLC27A3
SEMA3C	SLC35D2
SERPINB5	SLCO4A1

SFN	SMAGP
SLC7A5	SMARCA5
SLC9A3R1	SORBS2
SOCS3	SORT1
SPHK1	SPTBN1
SPRR1A	SULT1A1
SPRR1B	SYF2
STMN2	TACC2
STX1A	TAOK2
TFPI2	TGFBR2
TGFB2	TIMP3
TGFBI	TLR4
TIMP1	TMEM100
TMEM132A	TMEM106C
TNFRSF21	TMEM97
TPBG	TNS3
TRIB1	TOM1L1
TRIM29	TSPAN13
TSPAN5	TTC39A
TUBB2B	VAMP3
TUBB3	VPS13D
UCHL1	WASF3
ZFP36	WFS1
	YEATS2
	ZHX3
	ZNF185
	ZNF589
	ZNF75D

Supplemental Table 2. Sequences of gene-specific primers used for quantitative RT-PCR in murine samples.

Gene	Forward	Reverse
mHprt	GCCCTTGACTATAATGAGTACTTCAGG	TTCAACTTGCGCTCATCTTAGG
mIl-10	CAGAGCCACATGCTCCTAGA	GTCCAGCTGGTCCTTTGTTT
mCcr5	GAGACATCCGTTCCCCCTAC	GTCGGAACTGACCCTTGAAA
mCd44	CTCCTTCTTTATCCGGAGCAC	TGGCTTTTTGAGTGCACAGT
mCol1a1	AGACATGTTCAGCTTTGTGGAC	GCAGCTGACTTCAGGGATG
mCol5a	CTACATCCGTGCCCTGGT	CCAGCACCGTCTTCTGGTAG
mFn1	CGGAGAGAGTGCCCCTACTA	CGATATTGGTGAATCGCAGA
mαSma	TGACGCTGAAGTATCCGATAGA	CGAAGCTCGTTATAGAAAGAGTGG
mMmp-12	AATGCTGCAGCCCCAAGGAAT	CTGGGCAACTGGACAACTCAACTC
mHas2	GGCGGAGGACGAGTCTATG	ACACATAGAAACCTCTCACAATGC
mTimp1	GCAAAGAGCTTTCTCAAAGACC	AGGGATAGATAAACAGGGAAACACT
mCcl3	TGCCCTTGCTGTTCTTCTCT	GTGGAATCTTCCGGCTGTAG
mCcl20	GGTACTGCTGGCTCACCTCT	TGTACGAGAGGCAACAGTCG
mCdk4	AGAGCTCTTAGCCGAGCGTA	TTCAGCCACGGGTTCATATC
mIgf1	TCGGCCTCATAGTACCCACT	ACGACATGATGTGTATCTTTATTGC
mMycn	AGCACCTCCGGAGAGGATAC	CCACATCGATTTCCTCCTCT
mSphk1	ACAGTGGGCACCTTCTTTC	CTTCTGCACCAGTGTAGAGGC
mHsp90AA	GTCTCGTGCGTGTTCATTCA	CATTAACTGGGCAATTTCTGC
mHsp90AB	TACTCGGCTTTCCCGTCA	GCCTGAAAGGCAAAGGTCT
mMmp2	GGTGCTCCACCACATACAACT	CCCATGGTAAACAAGGCTTC
mMmp9	ACGACATAGACGGCATCCA	GCTGTGGTTCAGTTGTGGTG
mTimp2	CGTTTTGCAATGCAGACGTA	GGAATCCACCTCCTTCTCG

Supplemental Table 3. Sequences of gene-specific primers used for quantitative RT-PCR in human samples.

Gene	Forward	Reverse
hβ-actin	CCAACCGCGAGAAGATGA	CCAGAGGCGTACAGGGATAG
hCol1a	GGGATTCCCTGGACCTAAAG	GGAACACCTCGCTCTCCA
hFN1	CTGGCCGAAAATACATTGTAAA	CCACAGTCGGGTCAGGAG
hCol5a	CCTGGATGAGGAGGTGTTTG	CGGTGGTCCGAGACAAAG
hCD44	CAACAACACAAATGGCTGGT	CTGAGGTGTCTGTCTCTTTCATCT
hCCR5	GCCTCTGAATATGAACGGTGA	ACATTTCCCTTCGTTGCTTC
hMMP-12	AGTTTTGATGCTGTCACTACCG	CACTGGTCTTTGGTCTCTCAGAA
hCDK4	GTGCAGTCGGTGGTACCTG	TTCGCTTGTGTGGGTTAAAA
hIGF1	TGTGGAGACAGGGGCTTTTA	ATCCACGATGCCTGTCTGA
hSPHK1	TGAACCATTATGCTGGATATGA	TGTGCAGAGACAGCAGGTTC

Supplemental Table 4. Antibodies used for Immunostainings

Antibody	Dilution	Catlog#.	Company
HSP90	1:100	SC-7947	Santa Cruz Biotechnology
Vimentin	1:500	ab137321	Abcam
PCNA	1:2000	2586S	Cell signaling technology
Phalloidin-488	1:1000	12935S	Cell signaling technology
αSMA	1:20000	A5228	Sigma
Ki67	1:400	12202	Cell signaling technology

Supplemental Table 5. Antibodies used for Western blot

Antibody	Dilution	Catlog#.	Company
αSMA	1:20000	A5228	Sigma
FN1	1:500	SC-9068	Santa Cruz Biotechnology
FAK	1:1000	3285S	Cell signaling technology
pFAK	1:1000	3281S	Cell signaling technology

CDC42	1:1000	2466P	Cell signaling technology
RhoA	1:1000	2117P	Cell signaling technology
ERK	1:1000	SC-94	Santa Cruz Biotechnology
pERK	1:1000	SC-7383	Santa Cruz Biotechnology
HSP90*	1:1000	ADI-SPA-845-F	Enzo life sciences
GAPDH	1:5000	A300-641	Bethyl laboratories

References

1. Madala SK, Edukulla R, Schmidt S, Davidson C, Ikegami M, Hardie WD. Bone marrow-derived stromal cells are invasive and hyperproliferative and alter transforming growth factor-alpha-induced pulmonary fibrosis. *Am J Respir Cell Mol Biol* 2014; 50: 777-786.
2. Sontake V, Shanmukhappa SK, DiPasquale BA, Reddy GB, Medvedovic M, Hardie WD, White ES, Madala SK. Fibrocytes Regulate Wilms Tumor 1-Positive Cell Accumulation in Severe Fibrotic Lung Disease. *J Immunol* 2015; 195: 3978-3991.
3. Madala SK, Sontake V, Edukulla R, Davidson CR, Schmidt S, Hardie WD. Unique and Redundant Functions of P70S6K Isoforms Regulate Mesenchymal Cell Proliferation and Migration in Pulmonary Fibrosis. *Am J Respir Cell Mol Biol* 2016.
4. Kamal A, Thao L, Sensintaffar J, Zhang L, Boehm MF, Fritz LC, Burrows FJ. A high-affinity conformation of Hsp90 confers tumour selectivity on Hsp90 inhibitors. *Nature* 2003; 425: 407-410.